AIP Applied Physics Letters

# Physical and electrical properties of lanthanide-incorporated tantalum nitride for n -channel metal-oxide-semiconductor field-effect transistors

C. Ren, D. S. H. Chan, X. P. Wang, B. B. Faizhal, M.-F. Li, Y.-C. Yeo, A. D. Trigg, A. Agarwal, N. Balasubramanian, J. S. Pan, P. C. Lim, A. C. H. Huan, and D.-L. Kwong

Citation: Applied Physics Letters **87**, 073506 (2005); doi: 10.1063/1.1947901
View online: http://dx.doi.org/10.1063/1.1947901
View Table of Contents: http://scitation.aip.org/content/aip/journal/apl/87/7?ver=pdfcov
Published by the AIP Publishing

**Articles you may be interested in**

Oxygen incorporation and dipole variation in tantalum nitride film used as metal-gate electrode
J. Vac. Sci. Technol. B **30**, 042202 (2012); 10.1116/1.4729599

Strain induced changes in the gate leakage current of n-channel metal-oxide-semiconductor field-effect transistors
J. Appl. Phys. **110**, 014511 (2011); 10.1063/1.3603023

Work function thermal stability of Ru O 2 -rich Ru–Si–O p -channel metal-oxide-semiconductor field-effect transistor gate electrodes
J. Appl. Phys. **103**, 073702 (2008); 10.1063/1.2901016

NbO as gate electrode for n-channel metal-oxide-semiconductor field-effect-transistors
Appl. Phys. Lett. **84**, 4666 (2004); 10.1063/1.1759780

A 50-nm-gate-length erbium-silicided n-type Schottky barrier metal-oxide-semiconductor field-effect transistor
Appl. Phys. Lett. **84**, 741 (2004); 10.1063/1.1645665

This article is copyrighted as indicated in the article. Reuse of AIP content is subject to the terms at: http://scitation.aip.org/termsconditions. Downloaded to IP: 130.239.20.174 On: Mon, 24 Nov 2014 04:58:24

HTML ABSTRACT + LINKS

APPLIED PHYSICS LETTERS **87**, 073506 (2005)

# Physical and electrical properties of lanthanide-incorporated tantalum nitride for *n*-channel metal-oxide-semiconductor field-effect transistors

C. Ren, D. S. H. Chan,[a] X. P. Wang, B. B. Faizhal, M.-F. Li, and Y.-C. Yeo
*Silicon Nano Device Laboratory, Department of Electrical and Computer Engineering, National University of Singapore, Singapore 117576*

A. D. Trigg, A. Agarwal, and N. Balasubramanian
*Institute of Microelectronics, Science Park II, Singapore 117685*

J. S. Pan, P. C. Lim, and A. C. H. Huan
*Institute of Materials Research and Engineering, Singapore 117602*

D.-L. Kwong
*Department of Electrical and Computer Engineering, The University of Texas, Austin, Texas 78712*

(Received 25 January 2005; accepted 9 May 2005; published online 10 August 2005)

Lanthanide-incorporated tantalum nitride (TaN) is studied as a potential metal gate candidate for *n*-channel metal-oxide-semiconductor field-effect transistors (*n*-MOSFETs). Lanthanides such as terbium (Tb), erbium (Er), and ytterbium (Yb) are introduced into TaN to form $Ta_{1-x}Tb_xN_y$, $Ta_{1-x}Er_xN_y$, and $Ta_{1-x}Yb_xN_y$ metal gates, respectively, on $SiO_2$ dielectric. The resistivity, crystallinity, film composition, and work function of $Ta_{1-x}Tb_xN_y$, $Ta_{1-x}Er_xN_y$, and $Ta_{1-x}Yb_xN_y$ films were investigated at different post-metal-anneal temperatures and for different lanthanide concentrations. It was found that the work function of lanthanide-incorporated TaN can be effectively tuned by increasing the concentration of lanthanide. Work functions of about 4.2–4.3 eV can be achieved even after a 1000 °C rapid thermal anneal, making lanthanide-incorporated TaN a promising metal gate candidate for *n*-MOSFETs. The enhanced nitrogen concentration and the possible presence of lanthanide-N or Ta-N-lanthanide compounds in lanthanide-incorporated TaN film could be responsible for its chemical-thermal stability on $SiO_2$. © *2005 American Institute of Physics*. [DOI: 10.1063/1.1947901]

Scaling of complementary metal-oxide-semiconductor (CMOS) devices requires the metal gate electrodes to address the gate depletion, dopant penetration, and high gate resistance problems associated with the conventional polycrystalline silicon gate electrode. In order to satisfy the threshold voltage requirement, metal gates with work functions close to the conduction and valence bands of silicon are desired for *n*- and *p*-channel metal-oxide-semiconductor field-effect transistors (MOSFETs), respectively.[1] One of the major challenges in metal gate CMOS technology is the realization of a low work-function metal gate with good thermal stability for *n*-channel MOSFETs using a conventional gate-first CMOS process.[2,3]

Binary metal alloys, such as Ru-Ta and Ta-Ti, have been studied to achieve tunable work functions over a wide range.[4,5] However, thermal stability of these binary alloys tends to degrade when the concentration of the low work-function component increases. Refractory metal nitrides, such as tantalum nitride (TaN), hafnium nitride (HfN), and titanium nitride (TiN), have drawn considerable attention due to their excellent thermal and chemical stability.[6–8] Their work functions, nevertheless, are close to the midgap position of silicon, rendering the threshold voltage too high to be useful in bulk MOSFETs.

In this study, we report a novel approach to modify the work function of TaN by incorporating lanthanide elements (Tb, Er, and Yb) into TaN metal gate for *n*-channel MOSFETs. Incorporating lanthanide elements with low work functions can effectively lower the work function of TaN, and this allows the tuning of the metal gate work function by varying the concentration of lanthanide incorporated. Moreover, work-function values of about 4.2–4.3 eV can be

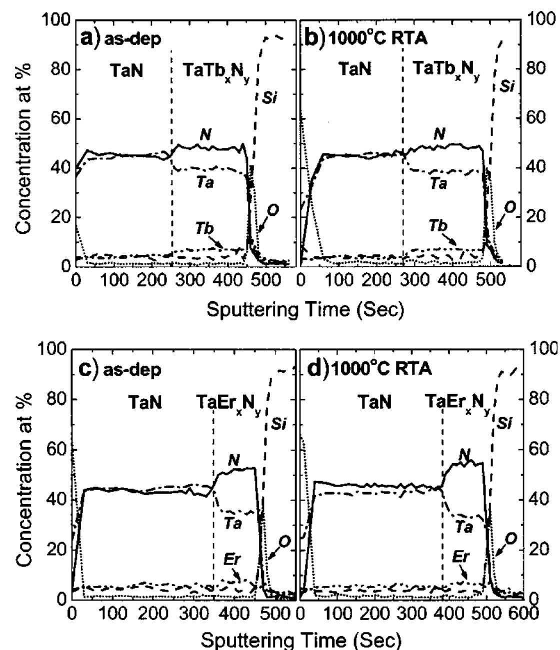


FIG. 1. AES depth profiling for $TaN/Ta_{0.94}Tb_{0.06}N_y/SiO_2$ (a,b) and $TaN/Ta_{0.95}Erb_{0.05}N_y/SiO_2$ (c,d) gate stacks before and after 1000 °C RTA in $N_2$ ambient.

[a]Author to whom correspondence should be addressed; electronic mail: danielchan@nus.edu.sg

This article is copyrighted as indicated in the article. Reuse of AIP content is subject to the terms at: http://scitation.aip.org/termsconditions. Downloaded to IP: 130.239.20.174 On: Mon, 24 Nov 2014 04:58:24

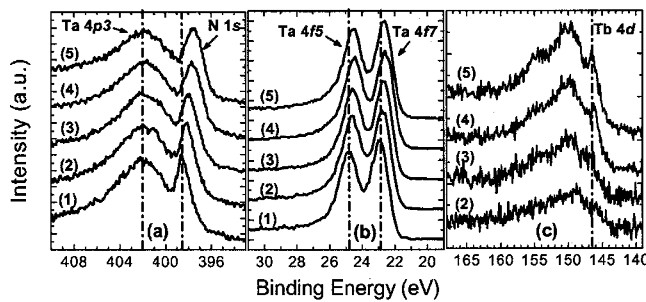


FIG. 2. The XPS spectra of the (a) N 1$s$, (b) Ta 4$f$, and (c) Tb 4$d$ region for the as-deposited $Ta_{1-x}Tb_xN_y$ films with different Tb concentrations: (1) TaN; (2) $Ta_{0.97}Tb_{0.03}N_y$; (3) $Ta_{0.94}Tb_{0.06}N_y$; (4) $Ta_{0.9}Tb_{0.1}N_y$; (5) $Ta_{0.87}Tb_{0.13}N_y$.

achieved after a rapid thermal anneal (RTA) process at 1000 °C, making lanthanide-incorporated TaN very attractive as a metal gate candidate for the gate-first CMOS process.[9] The resistivity, crystallinity, film composition, and binding characteristics of $Ta_{1-x}Tb_xN_y$, $Ta_{1-x}Er_xN_y$, and $Ta_{1-x}Yb_xN_y$ films are studied as functions of lanthanide concentration and annealing temperature. Thermal stability of the lanthanide-incorporated TaN with $SiO_2$ dielectric is also investigated.

MOS capacitors with various $SiO_2$ gate dielectric thicknesses were fabricated on $p$-Si (100) substrates (6–9 Ω cm). $Ta_{1-x}Tb_xN_y$, $Ta_{1-x}Er_xN_y$, and $Ta_{1-x}Yb_xN_y$ were deposited on thermally grown $SiO_2$ by reactive cosputtering of Ta and Tb (or Er, Yb) targets in a $N_2$ and Ar ambient. The sputtering power of the Ta target was kept at a constant value, while that of the Tb (or Er, Yb) target was varied to control the concentration of lanthanide in the TaN film. The $N_2$ and Ar flow rates were kept at 5 and 25 sccm, respectively, for all the films. *In situ* TaN capping layer with a thickness of ~1000 Å was deposited subsequently on top of all the lanthanide-incorporated TaN films to reduce the sheet resistance of the gate electrode stacks. The metal gate materials were then patterned by using $Cl_2$-based dry etching and followed by a wet etching process. Some of the devices were subjected to RTA at 800–1000 °C for 20 s in $N_2$ ambient for the evaluation of their thermal stability. Finally, all samples received a forming gas anneal at 420 °C for 30 min. Auger electron spectroscopy (AES), x-ray photoelectron spectroscopy (XPS), and x-ray diffraction (XRD) analysis were performed for material characterization. Sheet resistance of all the films was measured by a four-point probe. Capacitance-voltage ($C$-$V$) and current-voltage ($I$-$V$) characteristics were measured using HP4284 and HP4156A, respectively. Equivalent oxide thickness (EOT) and flatband voltage ($V_{FB}$) values were obtained by fitting the high-frequency $C$-$V$ curves with simulated $C$-$V$ curves produced by the QMCV program.[10]

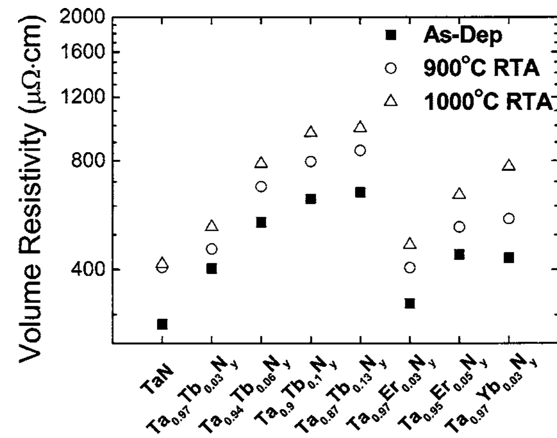


FIG. 3. Resistivity of lanthanide-incorporated TaN materials with different lanthanide elements before and after RTA at different temperatures in $N_2$ ambient.

The depth profile of the TaN/lanthanide-incorporated-TaN gate stack is studied by AES analysis. Figure 1 presents the AES results of the $TaN/Ta_{0.94}Tb_{0.06}N_y/SiO_2$ and $TaN/Ta_{0.95}Er_{0.05}N_y/SiO_2$ gate stacks before and after 1000 °C RTA. The Ta, Tb (Er), and N profiles appear to be very uniform across the TaN and $Ta_{0.94}Tb_{0.06}N_y$ ($Ta_{0.95}Er_{0.05}N_y$) films, without significant change observed before and after the 1000 °C RTA. It is found that the nitrogen concentration in $Ta_{0.94}Tb_{0.06}N_y$ (or $Ta_{0.95}Er_{0.05}N_y$) is remarkably higher than that in TaN film, which is observed from both the AES intensity profile and the concentration profile. Since the $N_2$/Ar flow and the Ta sputtering power during deposition are kept constant for both $Ta_{0.94}Tb_{0.06}N_y$ (or $Ta_{0.95}Er_{0.05}N_y$) and TaN films, this result implies that the presence of Tb (Er) enhances the nitrogen incorporation in $Ta_{1-x}Tb_xN_y$ (or $Ta_{1-x}Er_xN_y$) films. The reason needs to be further investigated. A plausible explanation could be that the lanthanide elements such as Tb and Er are more reactive than Ta so that it more easily combines with nitrogen. The higher N concentration may contribute to the thermal stability of lanthanide-incorporated TaN materials.

To study the effect of lanthanide on the binding energy of Ta and N in lanthanide-incorporated TaN films, XPS core-level spectra of N 1$s$, Ta 4$f$, and Tb 4$d$ regions for the as-deposited $Ta_{1-x}Tb_xN_y$ films with different Tb concentrations are shown in Fig. 2. The Tb/(Ta+Tb) ratios are determined from the Ta 4$f$ and Tb 4$d$ peaks. As shown in Fig. 2(a), the binding energy of the N 1$s$ peak shifts to lower energy as the Tb concentration increases, while that of the Ta 4$p_{3/2}$ peak

TABLE I. Work function and barrier height of lanthanide-incorporated TaN on $SiO_2$ as a function of rapid thermal anneal (RTA) temperatures.

| | Work function (eV) | | | | Barrier height (eV) | | | |
|---|---|---|---|---|---|---|---|---|
| Gate electrode | 420 °C | 800 °C | 900 °C | 1000 °C | 420 °C | 800 °C | 900 °C | 1000 °C |
| TaN | 4.4 | | 4.5 | 4.7 | 3.44 | | 3.5 | 3.73 |
| $Ta_{0.94}Tb_{0.06}N_y$ | 4.08 | | 4.15 | 4.23 | 3.12 | | 3.25 | 3.36 |
| $Ta_{0.95}Er_{0.05}N_y$ | 4.17 | 4.28 | 4.34 | 4.30 | 3.14 | 3.23 | 3.32 | 3.29 |
| $Ta_{0.97}Yb_{0.03}N_y$ | 4.44 | 4.34 | 4.36 | 4.37 | 3.40 | 3.25 | 3.41 | 3.05 |

This article is copyrighted as indicated in the article. Reuse of AIP content is subject to the terms at: http://scitation.aip.org/termsconditions. Downloaded to IP: 130.239.20.174 On: Mon, 24 Nov 2014 04:58:24

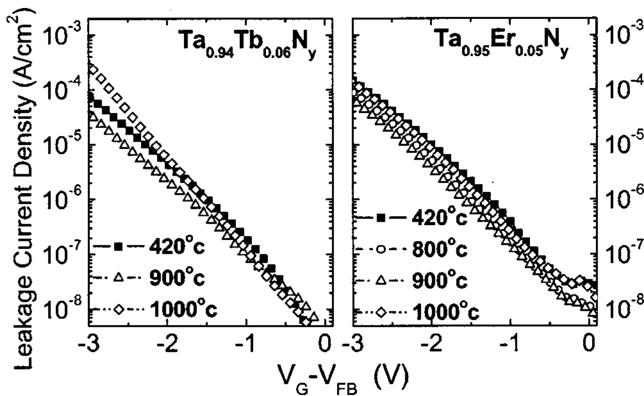


FIG. 4. Gate leakage characteristics of the $Ta_{0.94}Tb_{0.06}N_y/SiO_2$ and $Ta_{0.95}Er_{0.05}N_y/SiO_2$ MOS capacitors with post-metal anneal (PMA) performed at different temperatures. The oxide thickness is around $3.3 \pm 0.1$ nm.

remains almost constant. This implies that N may form new bonds with the incorporated Tb, either in the form of Tb-N or Ta-N-Tb compound, as the Tb concentration in $Ta_{1-x}Tb_xN_y$ increases. In Fig. 2(b), the Ta $4f_{7/2}$ peak in TaN shows a binding energy of 23.0 eV, which is higher than 21.9 eV for pure Ta, suggesting the existence of Ta-N bonds.[11] As the Tb concentration increases, the Ta $4f$ peak shows only a 0.3-eV shift which could be attributed to the formation of Ta-N-Tb compound. The signals from the Tb $4d$ peaks in Fig. 2(c) appear noisy due to the low Tb content. Similar results are observed in $Ta_{1-x}Er_xN_y$ and $Ta_{1-x}Yb_xN_y$, suggesting that lanthanide may form lanthanide-N or Ta-N-lanthanide compounds. Since the lanthanide elements are generally reactive, the compound formation with N may be helpful for improving the stability of the lanthanide in TaN.

The resistivity of lanthanide-incorporated TaN is evaluated as a function of RTA temperature. Note that the lanthanide-incorporated TaN films used for the resistivity studies are not capped with TaN. As shown in Fig. 3, the resistivity of lanthanide-incorporated TaN is higher than that of TaN and tends to increase with the increasing lanthanide concentration and RTA temperature. The higher resistivity of lanthanide-incorporated TaN compared with that of TaN could be due to the higher N concentration in the film. We have deposited $Ta_{0.9}Tb_{0.1}N_y$ films with fixed Ta/Tb sputtering power and a different $N_2$ flow rate. It is found that the film deposited in the ambient with a higher $N_2$ flow rate has a higher resistivity. It has been reported elsewhere that the resistivity of TaN and $TaSi_xN_y$ also increases with N concentration.[12,13] An increase of the resistivity with annealing temperature was also observed in our work, which is correlated with the oxygen traces in the $N_2$ ambient during the RTA process. The oxygen concentration in the $Ta_{1-x}Tb_xN_y$ films without a TaN capping layer was studied before and after 1000 °C RTA by AES analysis, and considerable increase in oxygen content was seen after RTA. The resistivity increase of the lanthanide-incorporated TaN films during RTA process could be suppressed with the use of a TaN capping layer. We have measured the sheet resistance of a $TaN/Ta_{1-x}Tb_xN_y$ stack before and after 1000 °C RTA and the sheet resistance of this stack could be kept below 20 Ω/□ after RTA.

Electrical characteristics of lanthanide-incorporated-$TaN/SiO_2$ gate stack are also examined under different RTA temperatures. Table I summarizes the work functions and barrier heights of several lanthanide-incorporated TaN electrodes on $SiO_2$. The work-function values are obtained from $V_{FB}$ versus EOT plots which excluded the impact of oxide fixed charges. The barrier height values are extracted by Fowler-Nordheim current analysis on capacitors with ~6 nm $SiO_2$ dielectrics.[14] The effective mass of 0.4 $(m_{ox}/m_0)$ was chosen for the tunneling electrons.[15] Most barrier height values correlate well with the extracted work-function values. Work-function values around 4.2–4.3 eV can be achieved by incorporating lanthanides into TaN even after a RTA process at 1000 °C. To evaluate the thermal-chemical stability of the lanthanide-incorporated-$TaN/SiO_2$ interface, *I-V* characteristics of $Ta_{0.94}Tb_{0.06}N_y/SiO_2$ and $Ta_{0.95}Er_{0.05}N_y/SiO_2$ stacks are measured after RTA at different temperatures, as shown in Fig. 4. The *I-V* characteristic does not show significant change after annealing at different temperatures, suggesting good thermal and chemical stability of the $Ta_{0.94}Tb_{0.06}N_y/SiO_2$ $(Ta_{0.95}Er_{0.05}N_y/SiO_2)$ interface. This might be attributed to the presence of N at the interface, which suppresses the diffusion or reaction of lanthanide with the underlying $SiO_2$.

In summary, lanthanide-incorporated tantalum nitride shows low work function and good thermal stability on $SiO_2$, making it attractive as a metal gate candidate for *n*-channel MOSFETs. The work function can be tuned by varying the concentration of the lanthanide. A work function of 4.2–4.3 eV can be achieved even after a 1000 °C RTA. The increased nitrogen concentrations in lanthanide-incorporated TaN films and the formation of Ta-N-lanthanide compounds could be important for the thermal and chemical stability on $SiO_2$.

[1] I. De, D. Johri, A. Srivastava, and C. M. Osburn, Solid-State Electron. **44**, 1077 (2000).
[2] Q. Lu, R. Lin, P. Ranade, T.-J. King, and C. Hu, Tech. Dig. VLSI Symp. **2001**, 45.
[3] T.-H. Cha, D.-G. Park, T.-K. Kim, S.-A. Jang, I.-S. Yeo, J.-S. Roh, and J. W. Park, Appl. Phys. Lett. **81**, 4192 (2002).
[4] J. H. Lee, H. Zhong, Y.-S. Suh, G. Heuss, J. Gurganus, B. Chen, and V. Misra, Tech. Dig. - Int. Electron Devices Meet. **2002**, 359 (2002).
[5] B.-Y. Tsui and C.-F. Huang, IEEE Electron Device Lett. **24**, 153 (2003).
[6] Y. H. Kim, C. H. Lee, T. S. Jeon, W. P. Bai, C. H. Choi, S. J. Lee, L. Xinjian, R. Clarks, D. Roberts, and D.-L. Kwong, Tech. Dig. - Int. Electron Devices Meet. **2001**, 667.
[7] D.-G. Park, Z. J. Luo, N. Edleman, W. Zhu, P. Nguyen, K. Wong, C. Cabral, P. Jamison, B. H. Lee, A. Chou, M. Chudzik, J. Bruley, O. Gluschenkov, P. Ronsheim, A. Chakravarti, R. Mitchell, V. Ku, H. Kim, E. Duch, P. Kozlowski, C. D'Emic, V. Narayanan, A. Steegen, R. Wise, R. Jammy, R. Rengarajan, H. Ng, A. Sekiguchi, and C. H. Wann, Tech. Dig. VLSI Symp. **2004**, 186.
[8] H. Y. Yu, J. F. Kang, J. D. Chen, C. Ren, Y. T. Hou, S. J. Whang, M.-F. Li, D. S. H. Chan, K. L. Bera, C. H. Tung, A. Du, and D.-L. Kwong, Tech. Dig. - Int. Electron Devices Meet. **2003**, 99.
[9] C. Ren, H. Y. Yu, X. P. Wang, H. H. H. Ma, D. S. H. Chan, M.-F. Li, Y.-C. Yeo, C. H. Tung, N. Balasubramanian, A. C. H. Huan, J. S. Pan, and D.-L. Kwong, IEEE Electron Device Lett. **26**, 75 (2005).
[10] K. J. Yang, Y.-C. King, and C. Hu, Tech. Dig. VLSI Symp. **1999**, 77.
[11] K. Sasaki, A. Noya, and T. Umezawa, Jpn. J. Appl. Phys., Part 1 **29**, 1043 (1990).
[12] C. S. Kang, H.-J. Cho, Y. H. Kim, R. Choi, K. Onishi, A. Shahriar, and J. C. Lee, J. Vac. Sci. Technol. B **21**, 2026 (2003).
[13] Y.-S. Suh, G. P. Heuss, V. Misra, D.-G. Park, and K.-Y. Lim, J. Electrochem. Soc. **150**, 79 (2003).
[14] Y.-S. Suh, G. P. Heuss, and V. Misra, Appl. Phys. Lett. **80**, 1403 (2002).
[15] M. Lenzlinger and E. H. Snow, J. Appl. Phys. **40**, 278 (1969).

This article is copyrighted as indicated in the article. Reuse of AIP content is subject to the terms at: http://scitation.aip.org/termsconditions. Downloaded to IP: 130.239.20.174 On: Mon, 24 Nov 2014 04:58:24